ISSN: 2710-0588

A Transmission Line Icing Detection Method based on Improved Canny and Hough Transform

Shilong Liu

College of Electrical Engineering, Southwest Minzu University, Chengdu 610041, China

Abstract

To address the issues of noise interference in edge detection of transmission line icing images and inaccurate thickness calculation due to scattered straight line detection, a detection method based on an improved Canny operator and optimized Hough transform is proposed. The Canny adaptive double threshold is achieved through the percentile sorting of gradient magnitude to enhance the robustness of edge extraction; the optimized Hough transform with line fitting is adopted to fuse scattered edges into complete icing edge lines ; and the thickness conversion is completed in combination with the camera imaging principle. Experiments show that this method can effectively improve the accuracy of icing thickness detection and has engineering application value.

Keywords

Detection of Ice Coating on Transmission Lines, Improved Canny Operator, Adaptive Double Threshold, Optimized Hough Transform, Camera Imaging Principle.

1. Introduction

Ice accumulation on transmission lines poses a serious threat to the safe operation of power grids, potentially leading to conductor galloping, line breakage, and even large-scale power outages[1]. In recent years, machine vision-based detection technology has attracted much attention due to its low cost, non-contact measurement, and flexible deployment [2]. However, traditional edge detection and line detection methods still face several challenges when applied to transmission line icing images.

The traditional Canny operator with fixed double thresholds is prone to missing or misidentifying ice edges under complex lighting and background conditions [3]. Meanwhile, the Hough transform may detect scattered icing edges as multiple discrete lines, which reduces the continuity of edge detection and affects the accuracy of icing thickness calculation [4].

To address these issues, this paper proposes a method for detecting the thickness of ice on transmission lines based on an improved Canny operator and an optimized Hough transform. The adaptive double thresholds of the Canny operator are determined through the percentile ranking of gradient magnitudes to enhance the robustness of edge extraction. Subsequently, an optimized Hough transform combined with line fitting is used to integrate scattered edges into complete icing edge lines. Finally, the icing thickness is calculated based on the camera imaging principle and the geometric relationship between image pixels and actual dimensions [5]. Experimental results show that the proposed method can effectively improve the accuracy and reliability of icing thickness detection, providing technical support for transmission line icing monitoring.

ISSN: 2710-0588

2. Edge Detection based on Improved Canny Operator

2.1. The Proposed Adaptive Dual-threshold Detection and Validity Verification Method based on Percentile Ranking

Double-threshold detection is the core step in Canny edge detection for screening valid edges and suppressing false edges, directly determining the integrity and accuracy of the detection results. The traditional Canny operator uses a manual threshold setting method, whose threshold values rely on subjective experience and cannot adapt to images with different noise intensities and gray-level distributions. It requires extensive repetitive experiments and debugging, and is prone to problems such as high thresholds causing the loss of weak edges and low thresholds retaining too many false edges, showing obvious limitations. Therefore, this paper proposes a method that can dynamically and flexibly set the double thresholds. This method consists of two important core parts, and the following focuses on explaining the processes and key steps of the two core parts.

2.1.1. The Gradient Magnitude Percentile Sorting Section

Percentile ranking is implemented based on the prctile function in MATLAB. The core is to locate the value corresponding to a specific percentile in the dataset and sort out the distribution pattern of gradient magnitudes. It is suitable for gradient magnitude datasets with continuous distribution and is specifically implemented in three steps:

a) Data sorting

Flatten the two-dimensional gradient magnitude matrix after non-maximum suppression into a one-dimensional vector, and then sort it in ascending order to obtain the sequence X_{sorted}.

During the sorting process, simultaneously record the correspondence between the gradient magnitudes and the original pixel coordinates to prevent confusion in subsequent edge localization.b) Determine the percentile index

Divide the sorted sequence into 100 equal intervals from 0 to 100 percentiles, and calculate the index k corresponding to each percentile p. The formula is as follows:

$$K = (\frac{p}{100}) \times (n+1) \tag{1}$$

In the formula, n represents the total number of elements in the one-dimensional gradient vector (the total number of pixels in the image). When k is an integer, the percentile takes the value of the element at the corresponding index in X_{sorted}; when k is not an integer, the percentile needs to be estimated through interpolation operation to ensure the accuracy of the boundary values of the interval.

c) Interpolation operation

The prctile function in MATLAB uses linear interpolation by default to handle non-integer indices. Let k = a + b (where a is the integer part and 0 < b < 1 is the fractional part). Select the elements corresponding to the adjacent integer indices a and a + 1, and calculate the weighted average to obtain the percentile P. The formula is as follows:

$$P = X_{sorted}[a] + b \times \left(X_{sorted}[a+1] - X_{sorted}[a] \right) \tag{2}$$

The gradient magnitudes corresponding to 100 percentiles can be accurately obtained through linear interpolation, providing reliable data for subsequent difference analysis and threshold location.

ISSN: 2710-0588

2.1.2. Part for Determining High and Low Thresholds

Based on the percentile ranking results, the difference calculation and threshold generation are completed by combining the diff function. Firstly, the gradient magnitudes corresponding to 100 percentiles are extracted to form the sequence P_p. The diff function is called to calculate the differences between adjacent percentiles, obtaining the difference sequence D_p. Utilizing the characteristic of sudden changes in gradient magnitudes in the edge regions, a difference threshold of 1 is set. The index P_h of the first difference greater than 1 is selected, and the corresponding gradient magnitude is set as the initial high threshold T_{high}. As shown in **Figure 1** shows the percentile gradient amplitude difference graph, with the percentile on the horizontal axis and the gradient amplitude difference on the vertical axis. It can be seen that the gradient amplitude difference shows a significant increase at the 94th percentile, and the difference is 1.023, which is greater than 1. After determining the percentile as 94%, the gradient magnitude in the corresponding sequence X_{sorted} is found based on its index and set as the high threshold. Then, 40% of the initial high threshold is taken as the initial low threshold T_{low}.

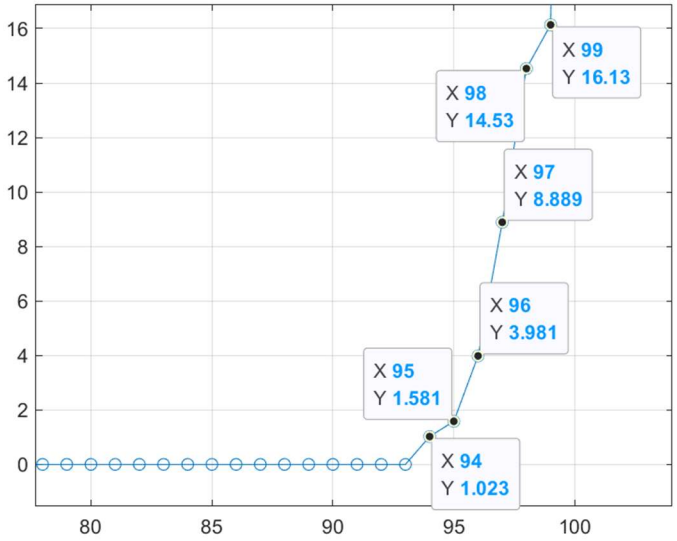

Figure 1. Percentile gradient magnitude difference map

2.1.3. Double-threshold Validity Check

To prevent the initial low threshold from being too low, the gradient magnitude corresponding to the first non-zero difference in D_p is extracted (i.e., the boundary value between noise and effective gradient). If the gradient magnitude is smaller than T_{low} by T_{low}, the high threshold T_{high} is updated to the magnitude corresponding to the next percentile, and the low threshold is recalculated and verified until T_{low} is greater than the gradient magnitude corresponding to the non-zero difference, obtaining the final double thresholds.

2.2. Edge Classification is Completed based on the Final Double Threshold.

Edges with gradient magnitudes greater than T_{high} are classified as strong edges, while those with magnitudes less than T_{low} are considered invalid edges (to be eliminated). Edges with magnitudes between these two thresholds are classified as weak edges (requiring further determination). The determination of weak edges is based on the continuity characteristics of real edges: real weak edges are often connected to strong edges, while pseudo-weak edges tend to exist in isolation. For each weak edge pixel, it is checked whether there is a strong edge within

ISSN: 2710-0588

its 3×3 neighborhood. If so, it is upgraded to a strong edge; otherwise, it is classified as an invalid edge. This approach makes the edge lines more continuous. Even if the gradient values in some areas are relatively weak, as long as they are adjacent to clear strong edge points, they can be regarded as part of the same edge. This method helps maintain the integrity of the edges and reduces the occurrence of breaks. **Figure 2** respectively show the three-dimensional images of the gradient magnitudes before and after edge determination. It can be clearly seen that after edge determination, many parts with gradient magnitudes lower than the low threshold at the bottom have been removed. This is because the valid edges have been retained and the invalid edges have been eliminated.

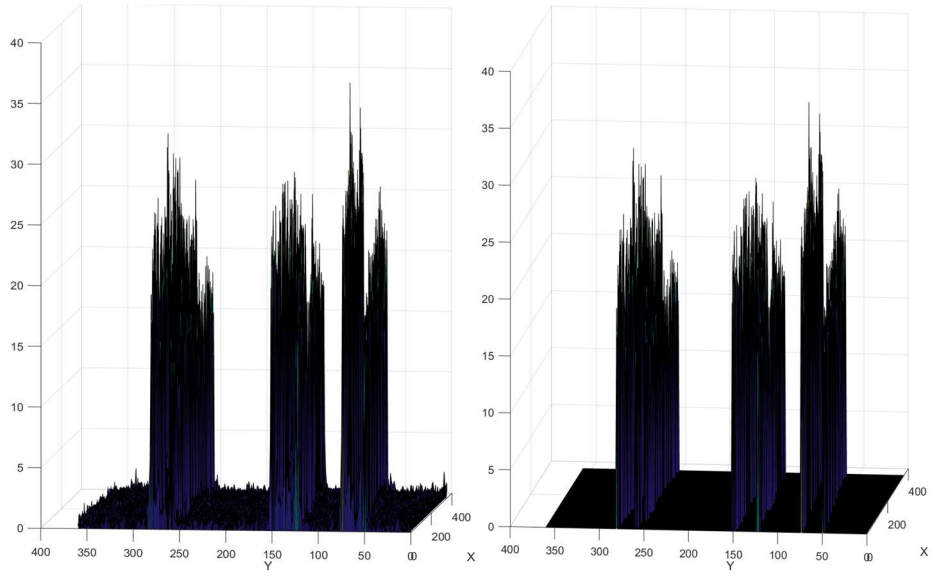

Figure 2. Comparison chart of 3D gradient magnitudes before and after edge determination

To verify the effectiveness of the above-mentioned improvement method, a comparison will be made between the traditional Canny detection and the improved dynamic double-threshold Canny detection. **Figure 3** shows the image after edge connection by adaptive double-threshold detection. It can be seen that after the adaptive double-threshold detection, the edges of the image are well preserved, the contours are clear, and most of the non-edge parts are eliminated.

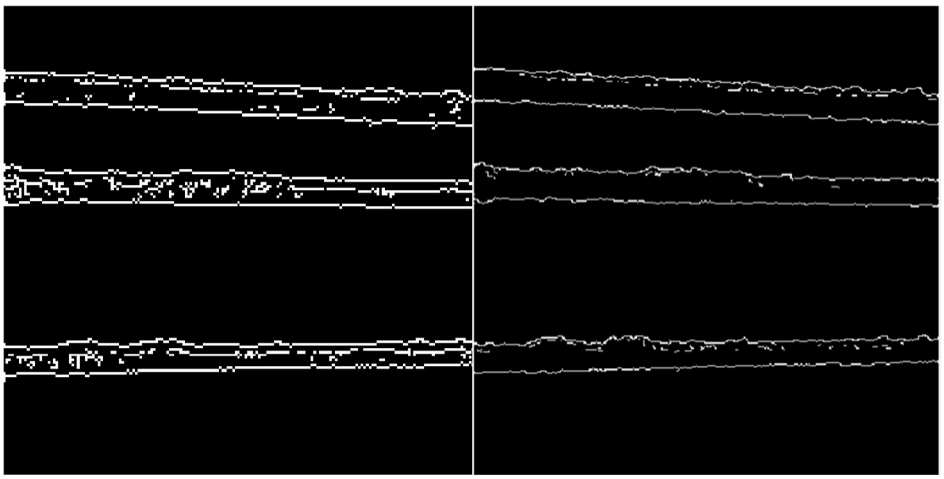

Figure 3. Comparison between conventional Canny detection and improved dynamic dual-threshold Canny detection

ISSN: 2710-0588

3. Line Detection based on Hough Transform

3.1. Selection of Straight Lines

After mapping the image space to the parameter space based on the Hough transform principle, the target straight lines are selected through accumulator voting and parameter quantization. Among them, the accumulator matrix is the core tool for straight line selection, used to record the number of votes corresponding to each (θ, ρ) parameter in the parameter space, and the quantization interval is used to simplify the calculation and optimize the algorithm performance.

The quantization interval is the step size that divides the continuous θ and ρ parameter spaces into discrete units in the Hough transform. Through parameter quantization, continuous parameters can be mapped to discrete units, effectively reducing the computational complexity, reducing the memory storage requirements, and improving the algorithm's operational efficiency and robustness. For example, if the quantization interval of ρ is set to a pixel and that of θ is set to b degrees, all ρ and θ values can be rounded to the nearest quantization unit to complete the parameter discretization process.**Figure 4** shows the result of the Hough accumulator.

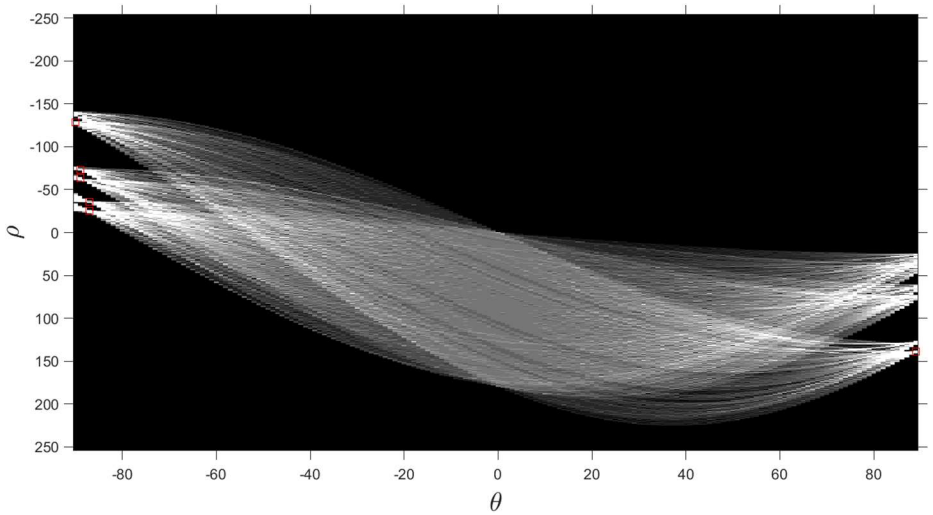

Figure 4. Hough accumulator result chart

3.2. The Proposed Linear Fitting Method

The straight lines detected by the Hough transform may have discontinuity and fragmentation issues. The main reason is that the actual shape of the transmission line is not an absolute straight line, and there may be local protrusions and edge fractures, which cause the collinear pixels not to be fully recognized, resulting in multiple discontinuous short lines, affecting the accuracy of the subsequent width calculation of the transmission line. Therefore, it is necessary to merge the discontinuous lines through the line fitting method to obtain a complete and continuous contour of the transmission line.

The core idea of line fitting is to set the matching conditions based on the parameter characteristics of the line, and merge the discontinuous short lines that meet the conditions into a complete line. First, select a reference line and set two key parameters: the tolerance of the offset angle and the tolerance of the offset distance, which are used to determine whether other discontinuous short lines are collinear with the reference line. Then, traverse all the short lines detected. If the offset angle and offset distance of a short line from the reference line are within the set tolerance range, it is determined that the two lines are collinear, and they are merged.

ISSN: 2710-0588

The starting point of the merged line is the starting point of the reference line, and the ending point is the ending point of the short line. Finally, repeat the above process to merge all the discontinuous short lines that meet the conditions into the reference line, and ultimately obtain a complete and continuous contour of the transmission line.

Figure 3-6 shows a comparison between the Hough transform detection results without linear fitting and those after linear fitting. It can be seen that the intermittent short lines have been effectively merged to form complete and accurate transmission line straight lines, providing reliable contour support for the subsequent calculation of the transmission line width, and simultaneously enhancing the integrity and accuracy of the straight line detection.

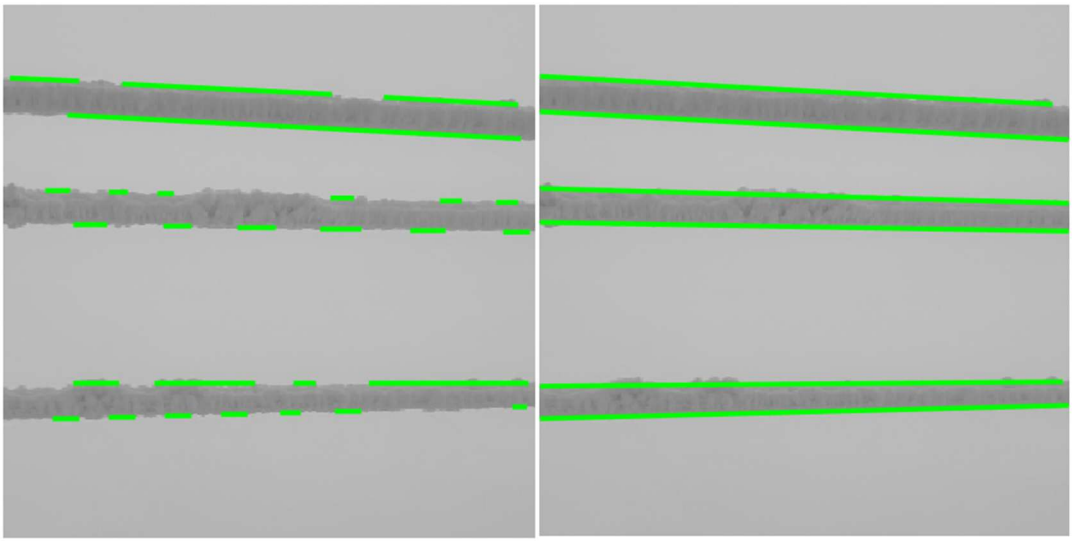

Figure 5. Comparison between Hough transform detection and straight line fitting results

4. A Calculation Model for Ice Thickness based on the Principle of Camera Imaging

4.1. The Principle of Camera Imaging

Figure 6 shows the principle diagram of camera imaging. Point A is the measured point, O' is on the optical axis Q (the center of the sensor, which is also the center of the image), with coordinates (U_0, V_0). Point A' is the image of point A on the sensor, with coordinates (U_1, V_1). Point P is the intersection point of the vertical line from point A to the plane where the optical axis Q lies, and point P' is the image of point P on the sensor, with coordinates (U_0, V_1). Point K is the projection point of the camera on the plane where point A lies, with a height of H. β_1 is the angle between line OP and the optical axis Q, ∂ is the angle between the horizontal line and the optical axis Q, f is the focal length of the camera, f_1 is the length of line OA', L is the length of line OP, D is the length of line KA, d is the length of line OA, D_y is the length of line KP, and D_x is the length of line AP.**Figure 7** is a top view of the sensor at V = V_1. In the figure, f_1' is the length of line OP', and β_2 is the angle between line OP' and OA'. Since the U-V coordinate system of the sensor plane represents the number of pixels, and the unit of the focal length f is mm, while the units of the pixel width and height are mm/pixel, for the subsequent measurement of the size of the transmission line, the focal length f and the pixel size are unified in units, that is, the length of O'P' is $(V_1 - V_0)dy$, and the length of P'A' is $(U_1 - U_0)dx$.

ISSN: 2710-0588

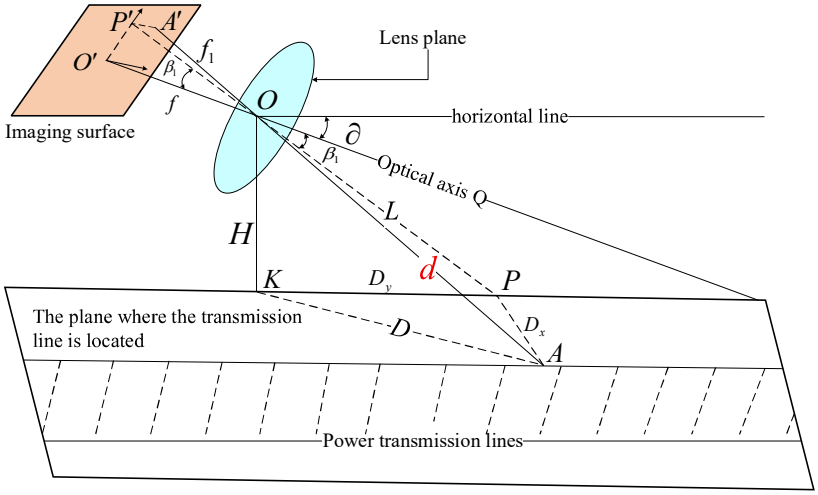

Figure 6. Camera imaging schematic

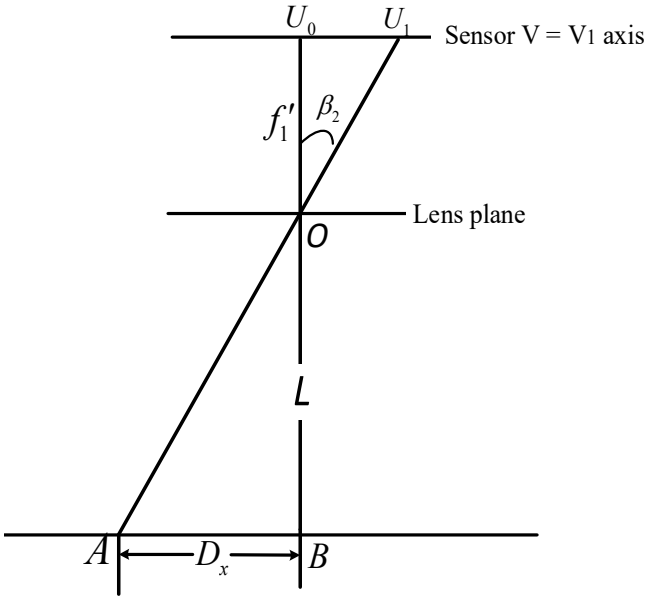

Figure 7. Top view of camera imaging geometry

Given the camera's assumed height H, setup angle ∂, focal length f, d_x and d_y, the following equation holds:

$$\tan\beta_1 = (V_1 - V_0)dy / f \tag{3}$$

$$\beta_1 = \tan^{-1}\frac{(V_1 - V_0)d_y}{f} \tag{4}$$

$$D_y = |KP| = H / \tan(\partial + \beta_1) \tag{5}$$

$$L = |OP| = H / \sin(\partial + \beta_1) \tag{6}$$

ISSN: 2710-0588

$$f_1' = \sqrt{(V_1 - V_0)^2 d_y^2 + f^2} \tag{7}$$

$$f_1 = |OA'| = \sqrt{(U_1 - U_0)^2 d_y^2 + (f_1')^2} \tag{8}$$

$$\tan \beta_2 = (U_1 - U_0) d_x / f \tag{9}$$

$$D_x = PA = L|\tan \beta_2| \tag{10}$$

$$D = \sqrt{D_x^2 + D_y^2} \tag{11}$$

$$D^2 = D_x^2 + D_y^2 = \frac{H^2 (U_1 - U_0)^2 d_x^2}{f^2 \sin^2(\partial + \tan^{-1} \frac{(V_1 - V_0) d_y}{f})} + \frac{H^2}{\tan^2(\partial + \tan^{-1} \frac{(V_1 - V_0) d_y}{f})} \tag{12}$$

$$d = |OA| = \sqrt{D^2 + H^2} \tag{13}$$

Among them, the pixel coordinate is $(U_i, V_i)(i = 0, 1, 2 \cdots i)$.

4.2. Calculation of Ice Thickness

After knowing the distance from the optical center to the test point, the camera's optical axis is set parallel to the transmission line. **Figure 8** shows the top view of its installation position, and **Figure 9** is the captured line diagram. A vertical line is drawn from point A to another line, with the vertical point being B. The imaging point of point A on the sensor is A', with the coordinate being (U_1,V_1). The imaging point of point B on the sensor is B', with the coordinate being (U_2,V_2). O' is on the optical axis Q (the center of the sensor), and its coordinate is (U_0,V_0).

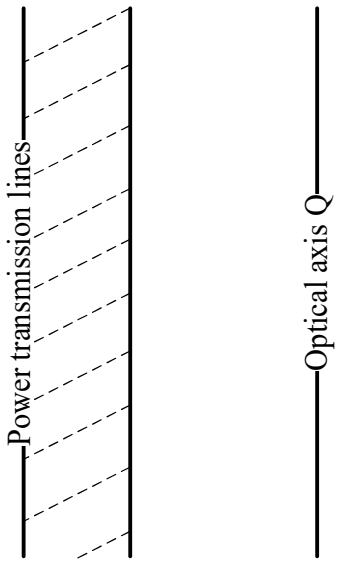

Figure 8. Top view of camera setup configuration

ISSN: 2710-0588

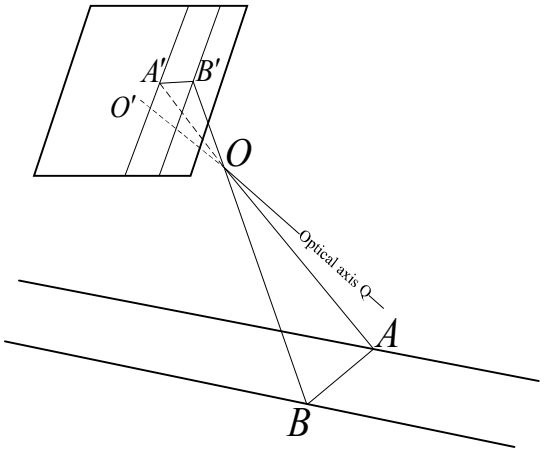

Figure 9. Image acquisition of transmission line

In Figure 3-18, the length of D_y can be obtained through Equations (3), (4), and (5), the length of D_x can be derived from Equations (6), (9), and (10), the length of line D can be calculated by Equation (10), and the length of line OA can be determined by Equations (12) and (13). The length of line OA' can be calculated by Equations (7) and (8). Due to the special shooting angle, line A'B' is parallel to line AB, and ΔABC is similar to ΔA'B'C'. Since the pixel coordinates of A' and B' on the image are known, the length of line A'B' can be obtained by the pixel size, thus:

$$\frac{OA}{OA'} = \frac{AB}{A'B'} \tag{14}$$

Since the coordinates of A' and B' are known, the length of the line A'B' can be obtained through the pixel size.

5. Experimental Results and Analysis

To verify the accuracy and feasibility of the method proposed in this paper, corresponding experimental analyses were designed and carried out. Considering the complex on-site environment of actual transmission lines, the high height of line erection, the limited shooting angle, and the randomness and suddenness of on-site icing scenarios, it is difficult to collect real icing images and the cost of sample acquisition is high, making it difficult to directly conduct large-scale on-site verification. Therefore, under the premise of ensuring the authenticity of the scene and the effectiveness of the method, this paper adopts a combination of indoor simulation and outdoor scenes to construct the experimental environment. Through scene simulation under controllable conditions, the proposed method is systematically tested and verified, thereby providing reliable experimental basis for subsequent practical engineering applications.

5.1. Indoor Model Wire Shooting

As shown in Figure 3-19, it is the indoor simulation scene of the ice-coated conductor and the original image captured. The ice-coated conductor is simulated by a plastic pipe wrapped with white cloth.**Table 1** lists the camera parameters and the experimental parameters measured by a vernier caliper. The camera used in this experiment is Canon EOS 60D, with a sensor size of approximately 0.86 inches (APS-C format). Based on the resolution and sensor size, it can be calculated that d_x = 22.3mm/5184 and d_y = 14.9mm/3456.

ISSN: 2710-0588

Table 1. Experimental parameters for indoor simulation of ice-coated conductor photography and measurement

Sensor size \mm	Resolution	f\mm	Camera mounting height \mm	Camera setup angle \°	Diameter of simulated transmission line \mm	Diameter of simulated ice-coated transmission line \mm
22.3×14.9	5184×3456	41	586.53	48	20	≈54.5

Figure 10. Indoor simulated ice-coated conductor shooting scene and original shooting images

Figure 11 shows the 3D graphs of gradient magnitudes before and after edge determination. By comparison, it is found that many small background interferences have been successfully removed after edge determination. **Figure 12** is the detection result graph of the improved Canny operator. **Figure 13** is the result graph of Hough transform line detection. It can be seen that the Hough transform line detection accurately detects two lines. **Figure 14** is the result graph of detection and thickness calculation based on the improved Canny and Hough transform. After recognition, the thickness is obtained as W ≈ 54.5936 mm, with an accuracy of 0.1 mm. This shows the feasibility and accuracy of this method.

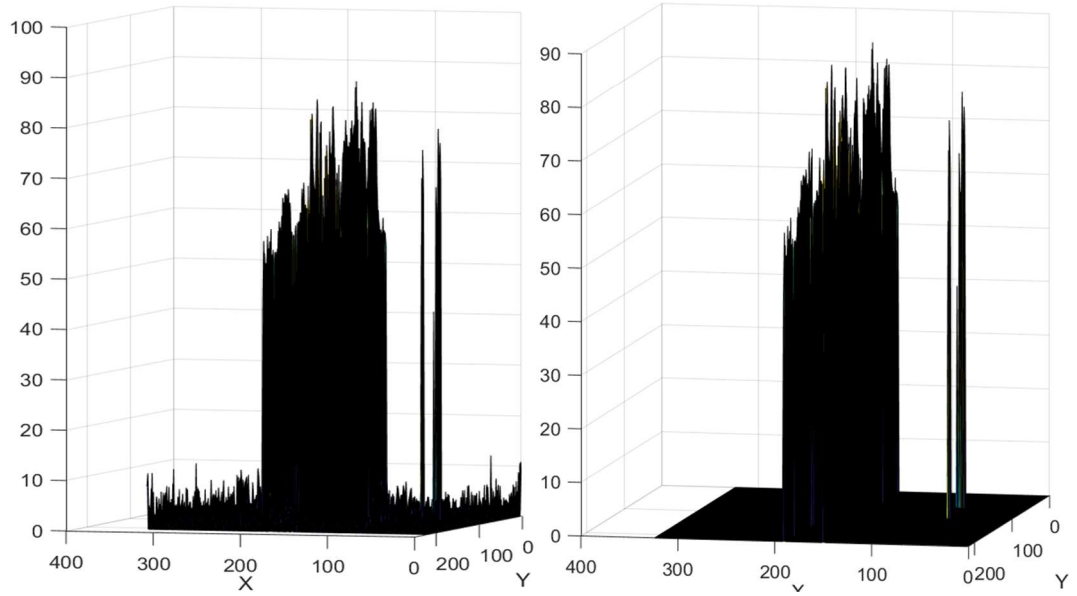

Figure 11. Comparison of indoor simulated ice-covered conductor images before and after edge determination

ISSN: 2710-0588

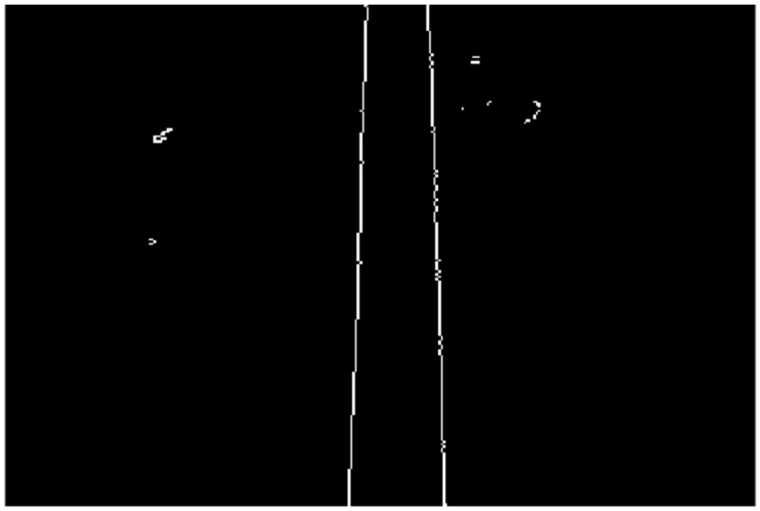

Figure 12. Detection result of indoor simulated ice-covered conductor using the improved Canny operator

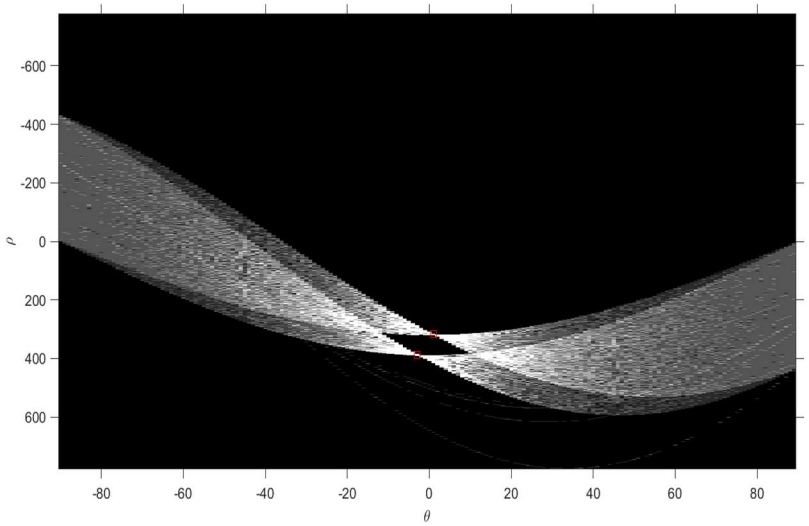

Figure 13. Line detection result of indoor simulated ice-covered conductor using Hough transform

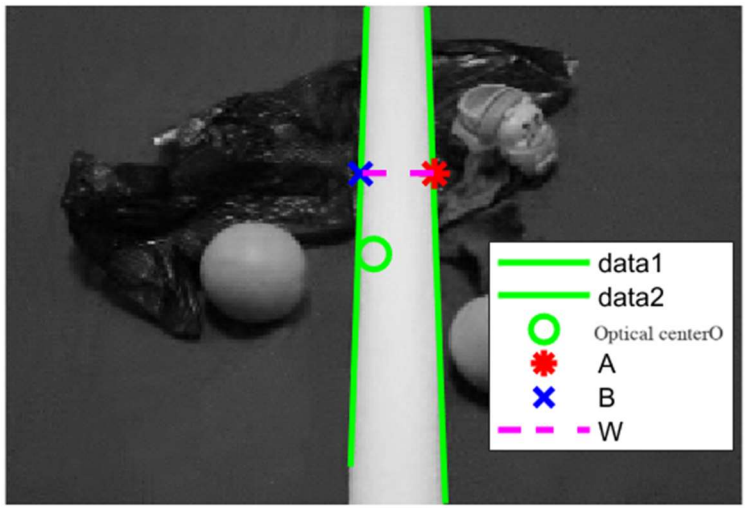

Figure 14. Detection result of indoor simulated ice-covered conductor based on the improved Canny algorithm and Hough transform

ISSN: 2710-0588

5.2. Outdoor Model Wire Shooting

As shown in **Figure 15**, it is the outdoor simulation scene of the ice-coated conductor and the original image captured. The ice-coated conductor is simulated by a plastic pipe wrapped with snow. **Table 2** shows the camera parameters and the experimental parameters measured by a vernier caliper. The camera used this time is the same as that used in the indoor shooting.

Table 2. Experimental parameters for outdoor simulated ice-coated conductor shooting and measurement

Sensor size \mm	Resolution	f\mm	Camera mount-ing height \mm	Camera setup an-gle \°	Diameter of sim-ulated transmi-ssion line \mm	Diameter o-f simulated ice-coated transmissi-on line \mm
22.3×14.9	5184×3456	40	1536.75	46	20	≈47.6

Figure 15. Outdoor simulated ice-coated conductor shooting scene and original shooting images

Figure 16 shows the 3D graph of gradient magnitude before and after edge determination. By comparison, it is found that **Figure 17** is the detection result of the improved Canny operator, **Figure 18** is the detection result of Hough transform for straight lines, and **Figure 19** is the detection and thickness calculation result based on the improved Canny and Hough transform.

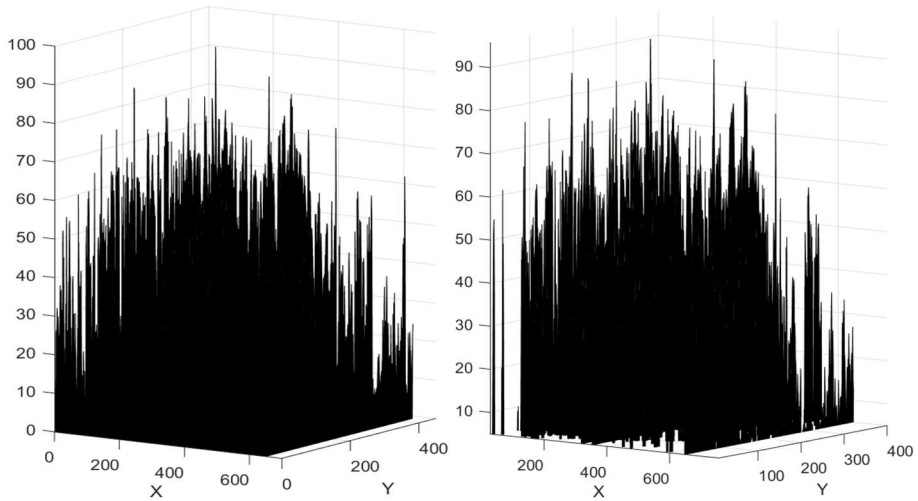

Figure 16. Comparison of outdoor simulated ice-covered conductor images before and after edge determination

ISSN: 2710-0588

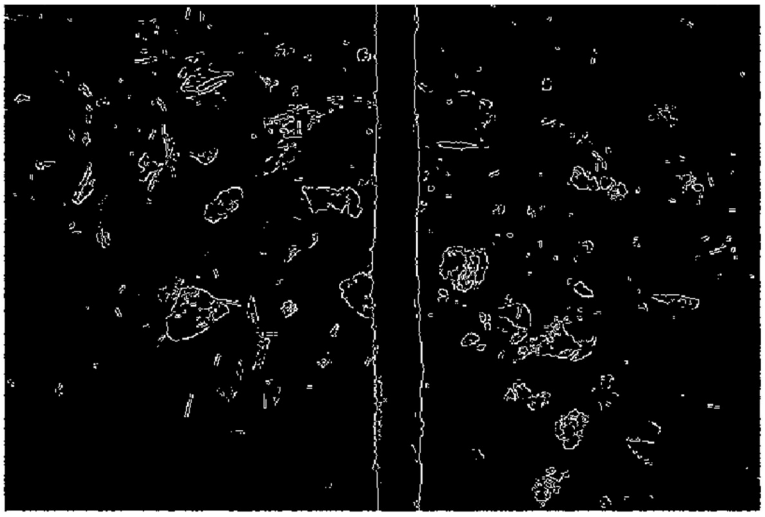

Figure 17. Detection result of outdoor simulated ice-covered conductor using the improved Canny operator

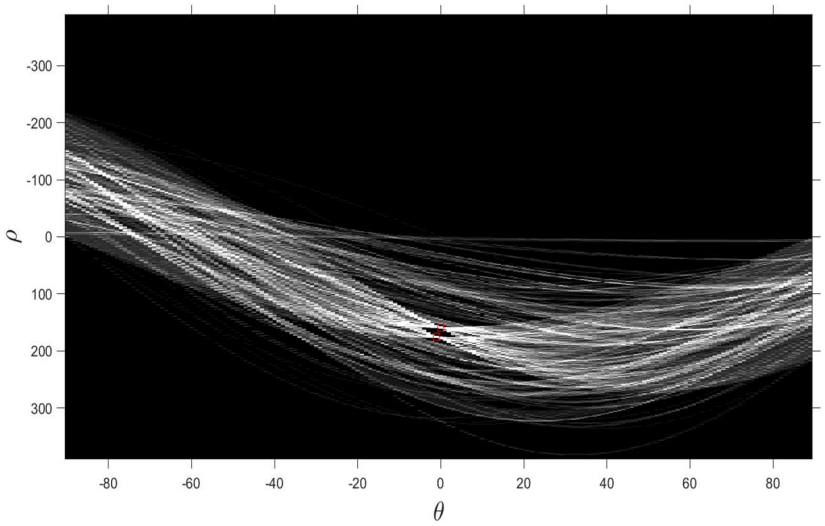

Figure 18. Line detection result of outdoor simulated ice-covered conductor using Hough transform

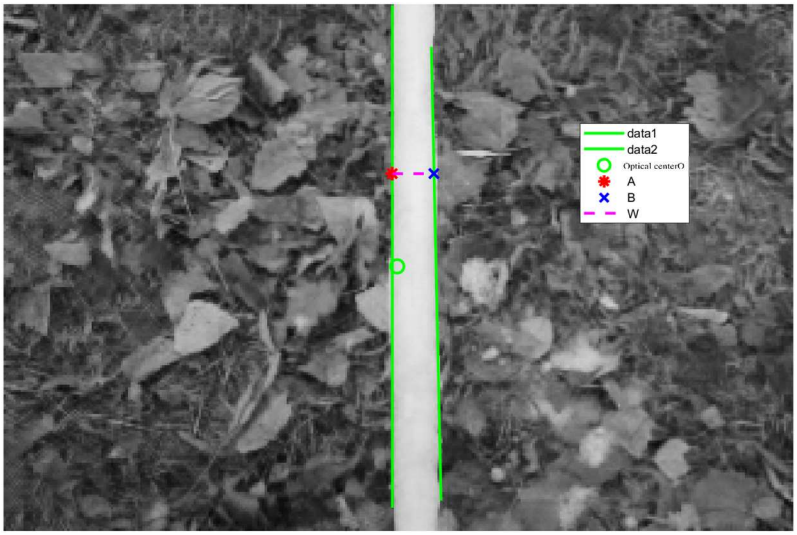

Figure 19. Detection result of outdoor simulated ice-covered conductor based on the improved Canny algorithm and Hough transform

ISSN: 2710-0588

5.3. Outdoor Model Wire Shooting

To quantitatively evaluate the performance of the proposed method in the task of detecting ice accumulation on transmission lines, comparative experiments were conducted in both indoor simulation scenarios and outdoor real-world scenarios. In the experiments, the actual diameter of the ice-coated conductor was taken as the reference standard. Firstly, n-fold downsampling (taking points every *n* pixels) was performed on the images in different scenarios for detection. The diameters of the simulated ice-coated conductors, the detection running time, and the detection errors for different sampling rates were statistically analyzed. The specific experimental results are shown in Table 3.

Table 3. Statistical results of downsampling at different multiples

Experimental scene	n	Diameter measurement result \mm	Detect running time	Detection error \mm
Indoor	4	54.623	17.3	<0.2
	8	54.895	8.7	<.0.5
	16	56.681	3.2	<2
	32	59.357	1.3	>4
outdoors	4	47.735.	19.5	<0.2
	8	47.924	9.6	<0.5
	16	49.327	3.5	<2
	32	51.266	1.3	>4

The downsampling experiment results of indoor and outdoor scenes show that as the downsampling factor n increases, the detection running time is significantly shortened, but the detection error also increases. When n ≤ 8, the detection accuracy is relatively high (error < 0.5mm), but the running time is longer; when n = 16, the running time can be compressed to 3-4 seconds under the premise that the error is controlled within 2mm, achieving a good balance between efficiency and accuracy; when n = 32, due to excessive loss of image details, the error exceeds 4mm, making it difficult to meet the requirements of ice thickness detection for transmission lines. Therefore, n = 16 is the better downsampling factor in this study that takes into account both detection efficiency and accuracy.

In summary, the transmission line icing detection method based on improved Canny and Hough transform proposed in this paper can quickly and accurately identify and calculate the diameter thickness of iced conductors when the background interference of the image is not severe. However, it still has certain limitations when dealing with severe background noise interference and uneven icing conditions. Therefore, the transmission line icing detection method based on YOLOv8 is proposed in Chapter 4 to make up for the existing deficiencies and shortcomings.

6. Conclusion

This paper proposes a method for detecting the thickness of ice-coated transmission lines based on an improved Canny edge detection and Hough transform. In response to the problems of traditional Canny edge detection operators in the application of transmission line images, such as the strong subjectivity of manual threshold setting, insufficient suppression of background noise, and poor edge refinement effect, this chapter proposes an adaptive double-threshold method based on percentile sorting, which effectively avoids the limitations of manual thresholds and significantly improves the accuracy and noise resistance of edge extraction in transmission line images. Secondly, this chapter optimizes the Hough transform

ISSN: 2710-0588

and line fitting methods, focusing on solving the problems of discontinuity and fragmentation of line contours that are prone to occur in traditional Hough transforms, and ultimately achieves the precise extraction of complete and continuous line contours of transmission lines. Combining the above image feature extraction results, this paper introduces the principle of camera imaging to construct an ice thickness calculation model, achieving the quantitative conversion from image features to actual ice thickness. Experimental verification results show that the detection algorithm system constructed in this chapter can well adapt to the actual scenarios of transmission line icing detection, with the accuracy of edge detection, the reliability of line contour extraction, and robustness in complex environments. At the same time, the calculation error of the ice thickness of ice-coated transmission lines based on the principle of camera imaging is small, with high accuracy and engineering application feasibility, fully verifying the practicality of this detection method.

Acknowledgments

The successful completion of this thesis would not have been possible without the constant companionship and support of my teachers, classmates and family. Here, I express my most sincere gratitude. I am deeply grateful to my supervisor, Ms. Wang Yan. From the selection of the topic, the construction of the framework to the revision of the content, you have always provided patient and meticulous guidance. Your rigorous academic attitude and pragmatic research spirit have greatly inspired me and will benefit me for a lifetime. I also thank my fellow students who have studied and strived together with me. During the research process, we exchanged ideas, encouraged each other and made progress together. This sincere friendship among classmates is warm and precious. I am also grateful to my family for their consistent understanding, support and silent dedication. You are my strongest backing, allowing me to focus on my studies and move forward with determination. I will always remember the gains and growth during this period of study. In the future, I will continue to be down-to-earth and dedicated to research with this sense of gratitude. I will not disappoint the teachings of my teachers and the expectations of my family. I will face the future with greater enthusiasm, constantly improve myself and strive for greater heights.

References

[1] L. Zhang, Q. Liu and H. Sun: Image-Based Monitoring Method for Transmission Line Icing Under Complex Backgrounds, Sensors, Vol.22 (2022) No.15, p.5824.

[2] M. Hu, J. He and M. Alsabaan: Image Identification Method of Ice Thickness on Transmission Line Based on Visual Sensing, Mobile Networks and Applications, Vol.28 (2023) No.5, p.1783-1792.

[3] Y. Yang, S. Hua, H. Wang, M. Li, Q. He, M. Zhao and Y. Wan: Detection Method of Icing Thickness of Overhead Transmission Lines Based on Canny Algorithm, International Journal of Energy Technology and Policy, Vol.19 (2024) No.3, p.344-362.

[4] W. Song, P. Li and M. Wang: Transmission Line Detection Based on Improved Hough Transform, Journal of Physics: Conference Series, Vol.2488 (2023) No.1, p.012045.

[5] X. Li, Y. Chen and Z. Zhao: Vision-Based Ice Thickness Measurement Method for Transmission Lines Using Edge Detection and Geometric Calibration, IEEE Access, Vol.10 (2022), p.118742-118751.